

# Variability in Blazars

Charles D. Dermer

*E. O. Hulburt Center for Space Research, Code 7653  
Naval Research Laboratory, Washington, DC 20375-5352*

---

## Abstract

The kinetic energy of bulk relativistic plasma ejected from the central engine of blazars is converted into nonthermal particle energy in the comoving frame through a process of sweeping up material from the surrounding medium. The resulting deceleration of the bulk plasma introduces a number of effects which must be included in blazar modeling. For example, the varying Doppler factor means that model fits must employ time integrations appropriate to the observing times of the detectors. We find that the ratio of the peak synchrotron fluxes reached at two different photon energies is largest when viewing along the jet axis, and becomes smaller at large angles to the jet axis. This effect is important in studies of the statistics of jet sources. Variability due either to bulk plasma deceleration or radiative cooling must be distinguished in order to apply recently proposed tests for beaming from correlated X-ray and TeV observations. The blast-wave physics developed to analyze these problems implies that most of the energy injected in the comoving frame is originally in the form of nonthermal hadrons. Because plasmoid deceleration can produce rapid variability due to a changing Doppler factor, arguments against hadronic blazar models related to the long radiative cooling time scale of hadrons are not compelling.

*Key words:* synchrotron emission; radio jets; X-rays and gamma-rays: spectra

---

Invited talk at VERITAS Workshop on TeV Astrophysics of Extragalactic Sources, Cambridge, MA, Oct. 23-24, 1998. In press, *Astroparticle Physics*, ed. M. Catanese, J. Quinn, T. Weekes

## 1 Introduction

Ejection of relativistic plasma from a compact central engine is thought to account for the appearance and observational properties of a number of fascinating systems in astronomy, including galactic black hole jet sources, radio

galaxies, quasars, and gamma-ray bursts (GRBs). Several arguments have led to this conclusion, perhaps the most important being measurements of apparent transverse superluminal motion in multi-epoch VLBI observations of radio quasars at the sub-pc scale. Apparent transverse speeds exceeding  $\sim 10c$  are found in many sources (e.g., Vermeulen & Cohen 1994). The interpretation of these observations in terms of bulk plasma outflow is not conclusive, however, as this effect could be related to the pattern speed of the emitting regions rather than to bulk plasma ejection. Another argument for relativistic plasma outflow yields a lower limit to the Doppler factor  $\mathcal{D}$  from the measured radio flux density, the angular diameter of the radio emission region, and the upper limit of the self-Compton X-ray flux (e.g., Marscher 1987; Ghisellini 1989). An accurate measurement of  $\mathcal{D}$  through this method requires contemporaneous radio and X-ray measurements and, moreover, an accurate determination of the radio self-absorption frequency. These conditions are met only rarely, but do point to relativistic motions in some flat-spectrum radio quasars.

Other tests for beaming try to establish conditions for the impossibility of intense, rapidly variable emission from stationary radiation sources. The argument of Elliot & Shapiro (1974) contrasts the range of allowed black hole masses for luminosities governed by Eddington-limited accretion, and variability time scales constrained by the light-travel time across a region with dimensions corresponding to the Schwarzschild radius of the black hole. A stationary, Eddington-limited emitting region is not possible if  $L_{48}/\Delta t(\text{days}) \gg 1$ , where  $10^n L_n \text{ ergs s}^{-1}$  and  $\Delta t(\text{days})$  are the observed luminosities and variability time scales in days, respectively. Klein-Nishina corrections must be applied (Dermer & Gehrels 1995) for observations at  $\gamma$ -ray energies.

Opaqueness of the emitting region to  $\gamma$ - $\gamma$  attenuation has also been used to argue in favor of beaming (Maraschi et al. 1992). In its simplest form, the constraint from the compactness parameter  $\ell = 4\pi m_e c^3 / \sigma_T = 6.6 \times 10^{29} \text{ ergs s}^{-1} \text{ cm}^{-1}$  implies that if  $L_{45}/\Delta t(\text{days}) \gg 1$ , then beaming is implied. Here the luminosity refers to emission near 1 MeV where the pair attenuation cross section is largest; consequently this test is most sensitive for observations near 1 MeV. Otherwise, assumptions about the cospatial origin of gamma rays and lower energy radiation must be justified by observations of correlated variability, since the cross section of  $\gtrsim 100$  MeV photons with each other is negligible (Dermer & Gehrels 1995).

Correlated X-ray and TeV observations of Mrk 421 (Macomb et al. 1995; Buckley et al. 1996) and Mrk 501 (Catanese et al. 1997) have demonstrated that 2-10 keV X-rays and  $\gtrsim 300$  GeV  $\gamma$  rays originate from the same region, verifying the cospatial assumption for these sources. Their luminosities are not large enough to establish beaming through  $\gamma$ - $\gamma$  transparency arguments, but can be used to determine the mean magnetic field  $H$  in the emitting region and establish a lower limit to the Doppler factor  $\mathcal{D}$  through a newly proposed

beaming test. This test is described in more detail below.

Because  $\gamma$ -ray observations probe the region nearest the black hole, it is important to critically examine these tests. An early hope was that such measurements could discriminate between accelerating and decelerating jet models (e.g., Marscher 1999) by charting the variation of  $\mathcal{D}$ , thereby revealing whether the evolution of a blazar flare is accompanied by a prompt phase of Doppler variation. The possibility that the Doppler factor of the emitting region can change, however, introduces intrinsic variability which must be distinguished from variability produced by radiative cooling of the emitting particles. It is therefore important to consider processes which change the bulk Lorentz factor of the radiating plasma. This is done in Section 2. In Section 3, we present numerical simulation results showing the effects of bulk plasma (or plasmoid) deceleration. Implications for beaming tests and blazar models are discussed in Section 4.

## 2 Blast-Wave Physics

Crucial for understanding variability behavior in blazars is to treat the injection of relativistic nonthermal particles in the comoving plasma fluid frame properly. The blast-wave physics developed to model GRB afterglows (e.g., Vietri 1997; Waxman 1997; Wijers et al. 1997) offers a solution to the particle injection problem, and provides a method to deal with the deceleration of the emitting plasma. The basic idea is that the energy of the injected nonthermal particles comes at the expense of the directed bulk kinetic energy of the fluid. The variation of the bulk Lorentz factor  $\Gamma$  of the radiating fluid can be simply obtained in a one-zone approximation through a momentum conservation equation (Dermer & Chiang 1998).

Suppose that the system produces an outflow with total energy  $E_0$  and initial bulk Lorentz factor  $\Gamma_0$ . Because most of the energy of the flow is bound up in the kinetic energy of baryons, assumed here to be protons, then  $E_0 = \Gamma_0 N_{\text{th}} m_p c^2$ , where  $N_{\text{th}}$  is the total number of protons. Thus  $\Gamma_0$  represents the baryon loading of the system.

It is straightforward to write a conservation equation for the radial (or  $\hat{x}$ ) momentum component of the fluid, given by

$$\Pi_x(x) = m_p c P \left\{ (1 + a) N_{\text{th}} + \int_0^\infty dp \cdot \gamma \cdot [N_{\text{pr}}(p; x) + a N_{\text{e}}(p; x)] \right\}, \quad (1)$$

where  $a \equiv m_e/m_p$ ,  $P \equiv B\Gamma = \sqrt{\Gamma^2 - 1}$ , and  $p = \beta\gamma = \sqrt{\gamma^2 - 1}$ . The functions  $N_{\text{k}}(p; x) \equiv dN_{\text{k}}(p; x)/dp$  represents the comoving distribution functions

of particles of type  $k = \text{pr}$  (protons) or  $k = \text{e}$  (electrons) at location  $x$ . This expression assumes no particle escape. Eq. (1) indicates that the momentum of the bulk plasma consists of both the inertia from the thermal protons associated with the baryon loading of the explosion, and the inertia bound up in the nonthermal proton and electron distributions. The latter functions evolve when nonthermal particles are injected into the plasma and when the energy of the nonthermal particles is radiated.

As a plasmoid or blast wave traverses the surrounding medium, it intercepts and sweeps up material. A proton and electron pair is captured by the plasmoid with a Lorentz factor  $\Gamma$  in the comoving plasma frame. The plasmoid captures protons and electrons from the surrounding medium at the rate

$$dN_{\text{pr,sw}}(p, x)/dx = dN_{\text{e,sw}}(p, x)/dx = n_{\text{ext}}(x)A(x)\delta(p - P), \quad (2)$$

The quantity  $n_{\text{ext}}(x)$  is the density of particles in the surrounding medium, and  $A(x)$  is the cross-sectional area of the plasmoid which is effective at sweeping up material from the external medium. The power of nonthermal particle kinetic energy injected into the comoving frame is simply

$$\dot{E}_{\text{ke}} = m_p c^2 \int_0^\infty dp (\gamma - 1) [\dot{N}_{\text{pr,sw}}(p, x) + a\dot{N}_{\text{e,sw}}(p, x)], \quad (3)$$

where the time derivative refers to time in the comoving frame. The distance  $\delta x$  traveled during the comoving time interval  $\delta t$  is  $\delta x = \delta t/(B\Gamma c)$ . Eqs. (2) and (3) therefore imply

$$\dot{E}_{\text{ke}} = m_p c^2 B\Gamma(\Gamma - 1)(1 + a)cn_{\text{ext}}(x)A(x) \quad (4)$$

(Blandford & McKee 1976). It is important to note that the fraction  $1/(1+a) = 99.95\%$  of the energy initially injected into the comoving frame is carried by protons, though plasma processes can be effective at transforming this energy to electrons or magnetic field.

By using eq. (1) to write  $\Pi_x(x + \delta x)$ , to which is added a term  $(d\Pi_x^{\text{rad}}/dx)\delta x$  to account for radiation losses, one obtains an equation of motion for the dynamics of the blast wave by expanding to first order in  $\delta x$  and using momentum conservation, i.e.,  $\Pi_x(x + \delta x) = \Pi_x(x)$ . It is

$$\frac{-dP(x)/dx}{P(x)} = \frac{n_{\text{ext}}(x)A(x)\Gamma(x)}{(1 + a)N_{\text{th}} + \int_0^\infty dp \cdot \gamma \cdot [N_{\text{pr}}(p, x) + aN_{\text{e}}(p; x)]}. \quad (5)$$

If external Compton scattering processes operate, an additional term must be added to take into account the momentum impulse from the scattered external photons (Böttcher & Dermer 1999).

Eq. (5) is the basic equation for calculating the dynamics of a plasmoid by

sweeping up material from the surrounding medium, and can be solved in a number of limiting cases. In the relativistic limit ( $\Gamma \gg 1$ ) and the blast-wave case where the area  $A(x) \propto x^2$ , there are two important regimes: the adiabatic (or non-radiative) and radiative regimes, where the swept-up particles retain all or none of their kinetic energy, respectively. Considering the simplest case where the density of the external medium can be parameterized by the expression  $n_{\text{ext}}(x) = n_0(x/x_d)^{-\eta}$ , one finds that  $\Gamma(x) \cong \Gamma_0$  for  $x \ll x_d$ , and  $\Gamma(x) \propto x^{-g}$  for  $x \gg x_d$ , where  $g = 3 - \eta$  and  $g = (3 - \eta)/2$  in the adiabatic and radiative regimes, respectively. The deceleration radius

$$x_d = \left[ \frac{(3 - \eta)E_0}{4\pi f_b n_0 \Gamma_0^2 m_p c^2} \right]^{1/3} \quad (6)$$

(e.g., Rees & Mészáros 1992), and represents the characteristic distance beyond which the behavior changes from a coasting solution to a decelerating solution. The term  $f_b$  represents the fraction of the full sky into which the explosion energy is ejected.

For intermediate radiative regimes where a fraction  $\zeta$  of the swept-up energy is retained in the blast wave, so that a fraction  $(1 - \zeta)$  is dissipated as radiation or lost through escape, Dermer et al. (1999) show that  $g = (3 - \eta)/(1 + \zeta)$ . In general, one may describe the dynamics of a blast-wave which decelerates by sweeping up material from a surrounding medium which is distributed according to the relation  $n_{\text{ext}}(x) \propto x^{-\eta}$  by an expression of the form

$$\Gamma(x) \cong \Gamma_0 / [1 + (x/x_d)^g] . \quad (7)$$

The relationship between the location  $x$  of the blast wave and the observing time  $t_{\text{obs}}$  can be obtained by noting that the radiating element travels a distance  $\delta x = \mathcal{D}\Gamma B c \delta t_{\text{obs}} / (1 + z)$  during the observing time interval  $\delta t_{\text{obs}}$ , where  $z$  is the redshift of the source,  $\mathcal{D} = [\Gamma(1 - B \cos \theta)]^{-1}$  is the Doppler factor, and  $\theta$  is the angle between the direction of motion of the radiating element (or the jet axis) and the observer's direction. From this relation, one can show that  $x \propto t_{\text{obs}}$  when  $x \ll x_d$ , and  $x \propto t_{\text{obs}}^{1/(2g+1)}$  when  $x \gg x_d$ .

The above expressions are sufficient to treat analytically the basic effects from blast wave deceleration and energization through the sweep-up process. Assuming that the fraction  $(1 - \zeta)$  of the swept-up power is dissipated in the form of radiation, then the radiated power in the comoving frame at  $x$  is  $\dot{E} \propto (1 - \zeta)\Gamma^2(x)n_{\text{ext}}(x)A(x)$ . The received power from a portion of the blast wave directed along the line-of-sight to the observer is equal to  $\dot{E}$  amplified by a factor  $\Gamma^2(x)/(1 + z)^2$  due to the transformations of energy and time. If the observer is outside the Doppler cone of the plasmoid, the emission is weak until the radiating plasma has slowed down sufficiently so that the Doppler cone intercepts the line of sight. At later times, the emission approaches the behavior found in the case where the observer's line-of-sight intercepts the

radiating region.

If  $\psi$  denotes the opening angle of the plasmoid (or jet), then two limits are important when the area of the plasmoid increases  $\propto x^2$ . From the above discussion, the received bolometric power  $P(t_{\text{obs}}) \propto (1-\zeta)\Gamma^4(x)n_{\text{ext}}(x)A(x)/(1+z)^2$ . The dynamics of the blast wave changes from a coasting solution to a decelerating solution when it passes the deceleration radius  $x_d$ , which occurs at the observing time

$$t_d = \Gamma_0(1 - B_0 \cos \theta)(1+z)x_d/(c\Gamma_0) \rightarrow (1+z)x_d/(2\Gamma_0^2 c); \quad (8)$$

here  $B_0 = \sqrt{1 - \Gamma_0^{-2}}$  and the right-hand expression of eq. (8) refers to the case when the plasmoid is directed along the line-of-sight.

For the case  $\theta \lesssim \psi$ ,  $P_p(t_{\text{obs}}) \propto t_{\text{obs}}^{2-\eta}$  when  $t_{\text{obs}} \ll t_d$ , and  $P_p(t_{\text{obs}}) \propto t_{\text{obs}}^{(2-\eta-4g)/(2g+1)}$  when  $t_{\text{obs}} \gg t_d$ . For observations at  $\theta \gtrsim \psi$ , the emission from the blast wave begins to intercept the observer's line-of-sight when  $\theta = 1/\Gamma(x)$ , which occurs when  $t_{\text{obs}} \approx t_d(\Gamma_0\theta)^{(2g+1)/g}$ . At this time, the received power is nearly equal to the value supposing that  $\theta \lesssim \psi$ .

We therefore see that the simplest model employing blast-wave physics shows how a plasmoid is energized by sweeping up material and converting it into nonthermal particle energy in the comoving frame (see Dermer et al. 1999 for more details). For a jet directed along the observer's line-of-sight (which is generally thought of as the standard model for blazars), the sweeping-up process produces a flare with bolometric flux rising  $\propto t_{\text{obs}}^{2-\eta}$ . After a sufficient amount of material has been swept up to cause the blast wave or plasmoid to decelerate, the Doppler deboosting overpowers the additional energization to cause the received flux to decay  $\propto t_{\text{obs}}^{(2-\eta-4g)/(2g+1)}$ . For adiabatic ( $g = 3/2$ ) and radiative ( $g = 3$ ) blast waves in a uniform surrounding medium with  $\eta = 0$ , the light curves decay  $\propto t_{\text{obs}}^{-1}$  and  $\propto t_{\text{obs}}^{-10/7}$ , respectively. The decaying flux is entirely a consequence of the decreasing Doppler factor. Thus it is not valid to interpret a decaying flux as evidence for cooling of the emitting particles without a discriminant between the effects of cooling and deceleration.

### 3 Numerical Calculations

Using the code described in Chiang & Dermer (1999), we can illustrate the effects described in the previous section for a pure synchrotron flare. In the simulation shown in Fig. 1, we let the central engine eject  $10^{48}$  ergs of plasma with a baryon loading given by  $\Gamma_0 = 40$  into 10% of the full sky. Thus the opening angle of the jet is  $11.5^\circ$ . The jet plasma passes through a medium with a uniform density of  $0.01 \text{ cm}^{-3}$ , and as it sweeps up this material it converts

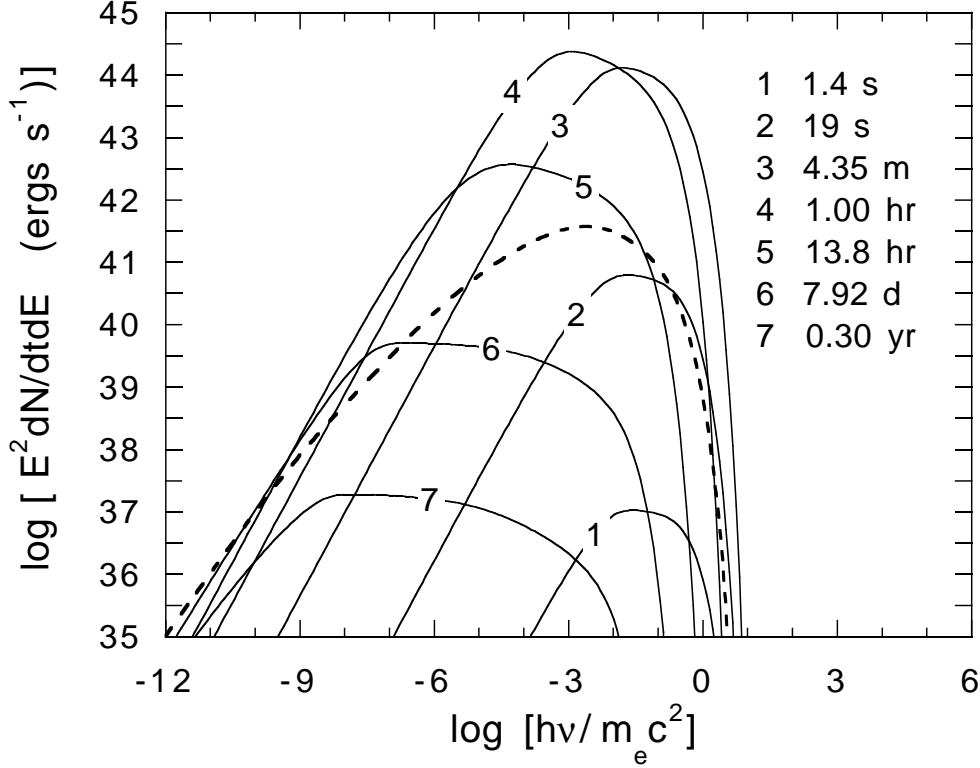


Fig. 1. Calculations of synchrotron spectra at times given by the labels on the figures. Observer is viewing down the jet axis. Parameters of the calculation are given in the text. Dashed curve shows the spectrum averaged over a one-day integration time.

it with high efficiency into nonthermal power-law electrons with a number injection index  $dN/d\gamma \propto \gamma^{-3}$ . The energy of the injected electrons ranges between  $\gamma = \Gamma$  and 1% of the maximum energy given by balancing the electron synchrotron loss time scale and the Larmor time scale in a magnetic field. We assume that the magnetic field energy density is 10% of the downstream energy density of the swept-up particles. This represents a magnetic field of 0.5 Gauss during the phase before the blast wave begins strongly to decelerate.

Electron synchrotron cooling is taken into account in the calculation, but makes only a small contribution to the variability shown here, which is due overwhelmingly to energization of the plasmoid by sweeping up particles, and to the subsequent deceleration and Doppler deboosting that results from this process. The general progress of the flare for the given parameters is to rise rapidly at X-ray and soft  $\gamma$ -ray energies. The flare then sweeps to lower energies on a much longer time scale. Note that the flare reaches larger  $\nu F_\nu$  peak fluxes at higher energies where it is most variable. At lower photon energies, the variability is less extreme, and the peak  $\nu F_\nu$  value reached is lower.

The dashed curve in Fig. 1 shows a one-day time integration over the flaring emission. As can be seen, the time-integrated spectrum is much softer than the time-resolved spectra because it represents a superposition of hard spectra

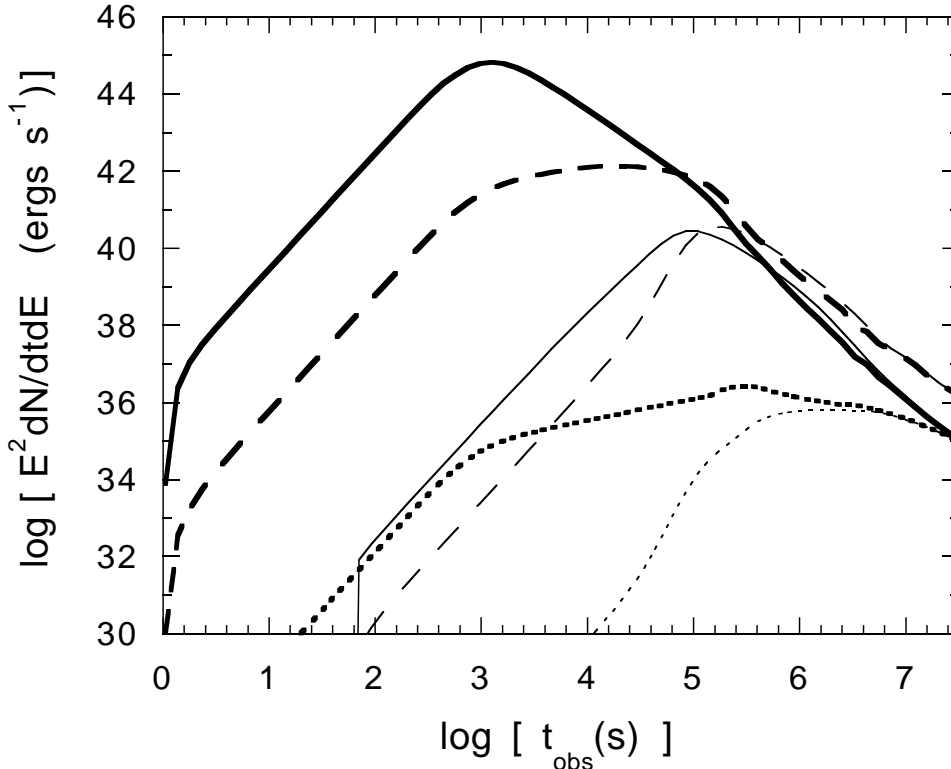


Fig. 2. Calculations of synchrotron flare light curves using the same parameters as in Fig. 1. Solid, dashed, and dotted curves are 1 keV X-ray, 1 eV optical, and 2.4 GHz radio light curves, respectively. Thick curves correspond to observations down the axis of the jet with opening angle  $\psi = 11.5^\circ$ , and thin curves represent observations at  $\theta = 20^\circ$  from the jet axis.

which peak at successively lower energies. When fitting blazar flare data using a model such as described here, it is therefore necessary to perform time-integrations over the flaring emission appropriate to the sampling time of the detector. Because gamma-ray telescopes require long observing periods to accumulate sufficient statistics, this is especially important for jointly fitting hard X-ray/soft  $\gamma$ -ray data, or MeV-GeV flares resulting from the synchrotron self-Compton (SSC) or external Compton scattering process.

Fig. 2 shows light curves for the model synchrotron flare shown in Fig. 1 at X-ray, optical and radio frequencies, both along the jet axis ( $\theta = 0^\circ$ ; thick curves), and at  $20^\circ$  to the jet axis (thin curves). When observing along the jet axis, the peak  $\nu F_\nu$  flux measured at higher frequencies is much greater than the peak  $\nu F_\nu$  flux measured at lower frequencies. By contrast, when observing outside the opening angle of the jet, i.e., when  $\theta > \psi$ , one sees that the range of peak fluxes becomes much less. Consequently, a flux-limited telescope observing at higher photon energies will be much more likely to detect beamed sources along the jet axis than a flux-limited telescope sensitive to lower energies,



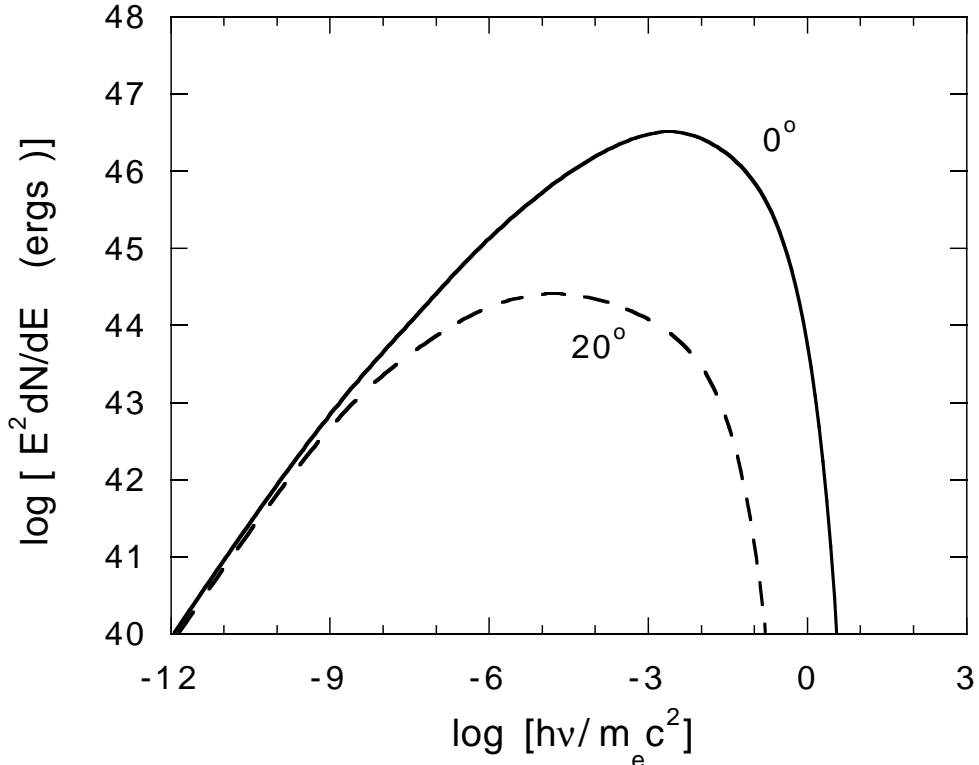


Fig. 3. Total energy received at different observing energies for the flare parameters shown in Fig. 1, for observations along the jet axis (solid curve) and at  $20^\circ$  off the jet axis (dashed curve). Flux-limited telescopes will preferentially detect jet sources along the jet axis when observing at the highest photon energies.

which will detect on-axis and off-axis sources with nearly equal likelihood.

This effect is a consequence of the energization and deceleration of the radiating plasma which causes the received emission to sweep to lower energies at late times, and has important implications for any statistical analyses of jet sources. In usual statistical treatments, one generally assumes that the relative flux observed at different angles to the jet axis is governed by the factor  $\mathcal{D}^{3+\alpha}$ , *independent of photon energy* (here  $\alpha$  is the energy index of the flux density  $F_\nu \propto \nu^{-\alpha}$ ; see, e.g., Urry & Padovani 1995). As shown here, the situation is much more complicated for flaring sources, which blazars most certainly are. A flux-limited X-ray survey primarily detects X-ray jet emission from aligned sources, with off-axis jet sources being too faint to detect at X-ray energies. By contrast, a flux-limited survey at radio energies will detect on-axis and off-axis sources at comparable flux levels. Thus we expect and do see the parent population of radio quasars, namely the radio galaxies. The parent population of X-ray selected BL Lac objects, by contrast, are at such a low flux level to hardly be detectable.

Fig. 3 shows the integrated energy fluence measured from a blazar flare at different photon energies, illustrating the effect just described. We have con-

sidered only the synchrotron emission up to this point, but the same behavior operates for the SSC flux (Dermer, Mitman, & Chiang 1999, in preparation). Variability will be greatest at higher photon energies, where the largest  $\nu F_\nu$  fluxes are reached for on-axis sources. The variability time scale will be longer and the flux roughly equal for aligned and misdirected blazars at lower photon energies. This same general behavior probably applies to external Compton scattering emission as well, though additional complications from the narrower beaming cone of ECS compared to the synchrotron and the SSC processes (Dermer 1995) must be taken into account in this case.

#### 4 Beaming Tests and Blazar Models

As noted in the Introduction, the correlated X-ray and TeV observations provide a new test for beaming in blazars. This test has been recently applied to observations of Mrk 501 by Catanese et al. (1997), Dermer (1998), and Kataoka et al. (1999). In this test, it is assumed that the X-ray emission is nonthermal synchrotron emission, and that the variability is a result of synchrotron losses in a magnetic field of mean intensity  $H$ . If the minimum variability time scale measured at energy  $\bar{E}$  is denoted by  $\delta t_{\text{obs}}^{\text{min}}$ , then

$$H(\text{G}) \cong 0.8 \left\{ \frac{(1+z)}{\mathcal{D}\bar{E}(\text{keV})[\delta t_{\text{obs}}^{\text{min}}(\text{hr})]^2} \right\}^{1/3}. \quad (9)$$

(e.g., Tashiro et al. 1995; Takahashi et al. 1996).

An upper limit on the mean magnetic field  $H$  in the emitting region is implied because the electrons producing the highest energy synchrotron emission have Lorentz factors  $\gtrsim 2 \times 10^6 E_C(\text{TeV})(1+z)/\mathcal{D}$ , where  $E_C(\text{TeV})$  is the measured energy in TeV of the highest-energy gamma-rays. Synchrotron emission correlated with the TeV flux requires that the electrons radiate in a magnetic field at least as great as  $H(\text{G}) \cong 11\epsilon_{\text{obs, syn}}\mathcal{D}/[E_C^2(\text{TeV})(1+z)]$ , where  $\epsilon_{\text{obs, syn}}$  is the measured dimensionless energy of the highest energy synchrotron photons produced by the electrons which produce the TeV radiation. When compared with the value of  $H$  inferred through equations (9), one obtains an expression for the Doppler factor, given by

$$\mathcal{D} \cong 1.7 \frac{(1+z)[E_C(\text{TeV})]^{3/2}}{\bar{\epsilon}_{\text{obs}}^{1/4}(\text{keV})(\delta t_{\text{obs}}^{\text{min}})^{1/2}(\epsilon_{\text{obs, syn}})^{3/4}} \quad (10)$$

(Dermer 1998). A lower limit to  $\mathcal{D}$  is obtained if the TeV flux does not exhibit a clear cutoff due to the high-energy cutoff in the electron distribution function.

With the advent of air Cherenkov telescopes such as Whipple and HEGRA detecting BL Lac objects to TeV and tens of TeV energies, this test could in

principle provide the largest inferred Doppler factors of all known beaming tests (J. H. Buckley, 1998, private communication). It is necessary, however, to discriminate clearly between bulk deceleration effects and radiative cooling effects. Unfortunately, the effects of deceleration mimic those of radiative cooling in a variety of ways (Chiang 1999). This is true both for the energy-dependent time lags produced by synchrotron cooling, and for the clockwise loop diagrams produced by flaring sources when data is plotted in a spectral index/intensity display (see also Kirk et al. 1999). One such discriminant might be the slower decay of the SSC emission compared to synchrotron emission (Dermer 1998), but a detailed numerical simulation will be required to fully resolve this question.

Finally, we note that the existence of the process of plasmoid deceleration weakens arguments (Buckley 1998) against hadronic models based on the long cooling time scales of protons through photo-meson, photon-pion, and proton synchrotron processes (e.g., Biermann & Strittmatter 1987) compared to the observed rapid variability time scales of BL Lacs. As shown here, neither extremely high energy protons nor intense radiation fields are required to produce rapid variability, which can result solely from Doppler deboosting due to the deceleration of the radiating region. This, and the fact that most of the nonthermal particle energy injected into the plasmoid is initially in the form of relativistic protons according to the blast wave physics described here, seems to give new life to hadronic models of blazars (e.g., Mannheim 1993; Gaisser et al. 1995) provided, of course, that hadronic models can successfully fit the generic two component  $\nu F_\nu$  blazar spectrum. If radiative cooling does not produce the variability behavior, hadronic models must also contend with low radiative efficiencies in an uncooled model (see Böttcher & Dermer 1998; Totani 1998 for related questions in GRB models). The variability behavior normally attributed to radiative cooling processes would, in the hadronic models, instead be a consequence of plasmoid deceleration. Thus a discriminant between cooling and deceleration effects is also of central importance to distinguish leptonic and hadronic models of blazars.

## 5 Summary

Recent observations of power-law X-ray afterglow observations of GRBs have stimulated the development of new physics for calculating radiation from relativistic plasma outflows. The energization of nonthermal particles in the radiating plasma occurs through a process of sweeping up material from the surrounding medium. The internal nonthermal particle energy is extracted from the directed kinetic energy of the bulk plasma, causing the bulk plasma to decelerate. We have examined idealized flaring behaviors produced when bulk plasma sweeps up particles from a uniform medium. Inhomogeneities in

the surrounding medium as well as in the relativistic plasmoid will complicate the situation.

We have shown that

- Bulk plasma deceleration effects must be included in models and statistical studies of blazars;
- Time integrations over the varying Doppler factor of the radiating plasma must be performed when fitting blazar data, employing integration ranges appropriate to the observing times of the different telescopes;
- A newly developed test for beaming in blazars using correlated X-ray and TeV variability observations must answer the criticism that the variability is due not to radiative cooling but rather to Doppler deboosting;
- Hadronic models for blazars do not have to confront the difficulty of the long radiative cooling time scales of hadrons, since variability can be achieved through plasmoid deceleration.

Important for further progress on these questions is an observational discriminant between cooling and deceleration processes.

## Acknowledgments

I acknowledge valuable discussions on blast-wave physics and synchrotron radiation with Jim Chiang, Markus Böttcher, and Hui Li, and thank Jim Chiang for the use of his code. This work was supported by the Office of Naval Research and the Compton Observatory Guest Investigator Program

## References

- [1] Biermann, P. L., & Strittmatter, P. A. 1987, *ApJ*, 322, 643
- [2] Blandford, R. D., & McKee, C. F. 1976, *Phys. Fluids*, 19, 1130
- [3] Böttcher, M., & Dermer, C. D. 1999, in preparation
- [4] Böttcher, M., & Dermer, C. D. 1998, *ApJ*, 499, L131
- [5] Buckley, J. H. et al. 1996, *ApJ* 472, L9
- [6] Buckley, J. H. et al. 1998, *Adv. Space Res.*, 21, 1/2, 101
- [7] Catanese, M. et al., 1997, *ApJ* 501, 616
- [8] Chiang, J., & Dermer, C. D. 1999, *ApJ*, in press
- [9] Chiang, J. 1999, *ApJ*, in press

- [10] Dermer, C. D., Chiang, J., & Böttcher, M., 1999, ApJ, 513, in press
- [11] Dermer, C. D., & Chiang, J. 1998, New Astronomy, 3, 157
- [12] Dermer, C. D., & Gehrels, N. 1995, 447, 103
- [13] Dermer, C. D. 1995, ApJ, 446, L63
- [14] Dermer, C. D. 1998, ApJ, 501, L157
- [15] Elliot, J. L., & Shapiro, S. L. 1974, ApJ, 192, L3
- [16] Gaisser, T. K., Halzen, F., & Stanev, T. 1995, Phys. Reports 258, 173
- [17] Ghisellini, G. 1989, MNRAS, 267, 167
- [18] Kataoka, J. et al. 1999, ApJ, in press
- [19] Kirk, J. G., Rieger, F. M., & Mastichiadis, A. 1998, A&A, 333, 452
- [20] Macomb D.J. et al. 1995, ApJ, 449, L99
- [21] Mannheim K., 1993, A&A, 269, 67
- [22] Maraschi, L., Ghisellini, G., & Celotti A. 1992, ApJ, 397, L5
- [23] Marscher, A. P. 1987, in Superluminal Radio Sources, ed. J. A. Zensus & T. J. Pearson (New York: Cambridge University Press), 280
- [24] Marscher, A. P. 1999, these proceedings
- [25] Rees, M. J., & Mészáros, P. 1992, MNRAS, 258, 41P
- [26] Takahashi, T. et al. 1996, ApJ, 470, L89
- [27] Tashiro, M. et al. 1995, PASJ, 47, 131
- [28] Totani, T. 1998, ApJ, 502, L13
- [29] Urry, C. M., & Padovani, P. 1995, PASP, 107, 803
- [30] Vietri, M. 1997, ApJ, 478, L9
- [31] Waxman, E. 1997, ApJ, 485, L5
- [32] Wijers, R. A. M. J., Rees, M. J., & Mészáros, P. 1997, MNRAS, 288, L51
- [33] Vermeulen, R. C., & Cohen, M. H. 1994, 430, 467